אוניברסיטת בן גוריון בנגב

הצעת תוכנית מחקר ללימודי דוקטורט

שרידות וניידות במערכות דלילות מזוגגות

Survival and Transport in Glassy Sparse Systems

Yaron de Leeuw

ירון דה ליאו

21.10.2012

חתימת מנחה: _____

חתימת יו"ר ועדת מוסמכים מחלקתי: _____

תקציר

אנו חוקרים הסעה והתפשטות ברשתות דלילות לא מסודרות. בתחילה, לכל אתר משויך מיקום מרחבי. אנו משתמשים במטריצת המרחקים בין הנקודות כבסיס להגדרת משוואות קצב או המילטוניאנים. בנוסף לכך, המטריצה יכולה להיות תלויה במשתנה צימוד המשויך לקשתות (החיבורים שבין האתרים). לפיכך, על ידי הגרלת מיקום האתרים או משתני הצימוד, אנו יכולים לגרום לאי סדר במערכת.

אם המשתנים השונים בבעיה שונים בסדרי גודל, כאשר רובם קטן מאוד ביחס לקבוצה מצומצמת, ניתן לקרוא לרשת דלילה. תחום העניין המרכזי שלנו הוא תכונות ההסעה ארוכות הטווח במערכות דלילות אלה.

שתי גישות עיקריות מובילות אותנו בבואנו לחקור את תכונות ההסעה, הן הגישה דרך התכונות הספקטרליות של המטריצה, והן דרך אנלוגיה לרשתות נגדים חשמליות. במערכות סטוכסטיות חד ממדיות, הדלילות גוררת תת-דיפוזיה, בעוד במערכות ממימד גבוה יותר הדיפוזיה נשארת רגילה, אך מקדם הדיפוזיה קטן כתוצאה מהדלילות.

על ידי שילוב רעיונות משיטת "דילוג הטווח המשתנה" (VRH) ורעיונות מתחום תורת הפרקולציה, הצענו שיטה בשם "דילוג הטווח האפטקיבי" (ERH) על מנת להעריך את מקדם הדיפוזיה.

אנו משווים תוצאות חישוביות למקדם הדיפוזיה עם הקירוב הלינארי ועם קירוב "דילוג הטווח האפטקיבי".

אנו דנים בהרחבות נוספות, ובכללן מספר מרובה של חלקיקים, וגרסא דו מימדית למודל סיני (Sinai).

Abstract

We study transport and spreading in sparse disordered networks. The networks are constructed by assigning spatial locations to sites. Distance matrices (also called Euclidean Distance Matrices) form the basis to define either rate equations or Hamiltonians. Additionally, the matrix might depend on some coupling parameter assigned to each network edge. Thus, by randomizing either the locations of the sites or the coupling parameter, we can induce disorder.

By allowing the network elements to differ by orders of magnitude, with most of the elements vanishingly small, we create a "sparse" network. Our interest lies in the long term transport properties of these sparse systems.

We approach the subject of transport by looking at the spectral properties of these networks, as well as by their resistor network analogies. For stochastic systems we see that in pure $1d$ this sparsity causes subdiffusion, while in quasi $1d$ and higher dimensions the system remains diffusive but with a reduced diffusion coefficient.

The *ERH - Effective Range Hopping* - method is suggested to estimate this diffusion coefficient by combining ideas from the well established *VRH* scheme with ideas from percolation theory.

The numerical results for the diffusion coefficient are compared to the linear estimate and to the improved *ERH* result.

Further generalizations are discussed, including multiple interacting particles and an assymetric version to the VRH procedure. Another proposed model is a $2d$ variant of the Sinai model.

Contents

Part I

Research Proposal

Chapter 1

Introduction

This proposal is about simple dynamical networks, with dynamics that are described either by a stochastic rate equation

$$\frac{dp_n}{dt} = \sum_m w_{nm} p_m \tag{1.1}$$

or by the Schrödinger equation:

$$\frac{d\psi_n}{dt} = \sum_m \mathcal{H}_{nm} \psi_m \tag{1.2}$$

Regardless of the governing equation, the focus is on disordered sparse networks, with wide distribution of energies. Two related aspects of these networks will be studied: their energy spectrum, and their spreading properties. More specifically, we wish to determine whether the networks are diffusive ($S(t) \sim t$), or sub-diffusive, and if they are indeed diffusive, what is the diffusion coefficient.

To simplify the discussion, we concentrate on d-dimensional spatial networks, in which each node has a defined location x_n, and each edge has an associated energy barrier ϵ_{nm}. The transition rates are then defined to be:

$$w_{nm} = w_0 \mathrm{e}^{-\epsilon_{nm}} B(x_n - x_m) \tag{1.3}$$

Where $B(r)$ describes the dependence of the coupling on the distance between sites.

The model we start with has its sites distributed randomly and uniformly throughout a d-dimensional hypercube, with $B(r) = \exp(-r/\xi)$. The disorder is defined by the location of the sites, and its effect on the connectivity of the network can be manipulated through the parameter ξ.

1.1 Matrices of interest

Our focus is on real-valued matrices. This ensures that the eigenvalues are either real or pairs of complex conjugates. This reminds us of Hamiltonians that conserve PT (Parity-Time) reversal symmetry. Actually, by change of basis, these Hamiltonians can probably be presented as real valued matrices.

These real matrices span several categories:

1. Active network : these matrices have negative and positive off-diagonal values
2. Detailed balance network: these have positive off-diaonal elements that satisfy the specific ratio $w_{nm} = \exp\left(-\frac{E_n - E_m}{T}\right) w_{mn}$
3. Symmetric network: these matrices have positive symmetric off-diagonal elements $w_{nm} = w_{mn}$. This can be regarded as the $T \to \infty$ limit of the previous category.
4. Other: these do not obey detailed balance.

The active networks (1) are called so because they can not be realized using passive elements such as resistors or capacitors only. The detailed balance networks (2) allow the system to reach Boltzmann's equilibrium, while the symmetric matrices (3) have the very useful analogy to a simple resistor network. Another important topic is the diagonal. For some networks, the natural definition of the diagonal is by demanding the sum of each row to be equal to zero (meaning $w_{nn} = -\sum_{m \neq n} w_{mn}$). This represents conservation of charge, probability or momentum in the model, and creates a special mode with $\lambda = 0$ and equal site probabilities, which has important consequences regarding localization (see 1.3). Another common practice regarding the diagonal is using some random distribution for it.

The old text:

In general, the transition matrices have three symmetry categories:

- $w_{nm} = w_{mn}$ - In the symmetric case the system could reach equilibrium and ergodicity. The transient behavior might be diffusive. This kind of system has the analog of a Resistor Network, which is often useful both analytically and numerically.
- $w_{nm} = \exp -\frac{E_n - E_m}{T} w_{mn}$ - This is called detailed balance, and allows the system to reach Boltzmann's equilibrium. One could make the analogy of a "stochastic field",

$\varepsilon(x) = \frac{E_n - E_m}{T}$. Any closed loop integral over such a field must equal zero. Note that any product of a symmetric operator with a diagonal operator can be said to satisfy detailed balance [1]

- $w_{nm} \neq w_{mn}$ - In the assymetric case, a Non Equilibrium Steady State (NESS) might be reached.

1.2 Motivations for the model

We have kept the model abstract and general on purpose, so that it might fit a large number of physical situations. Some physical applications include:

- Balls and Springs - A simple mechanical system of balls connected to each other by springs. The vibrational modes of the system are phonons, which conduct heat.
- Capacitors and Resistors - An electrical network of capacitors connected to each other by resistors.
- Mott impurity hopping - This kind of conductance arises from hopping between impurities.

1.3 The Anderson localization

In the Anderson model[2], a nearest neighbor network is formed on a lattice. The bonds are all equal, and the on-site energies are random. For $d = 1$ and $d = 2$, all states are localized, while for $d > 2$, there exists a transition between localized and extended modes.

There are several routines used to distinguish between exponentially localized and delocalized modes. The most straight forward one seems to be the participation number (PN) [3], which is defined by its inverse:

$$PN^{-1} = \sum_i p_i^2 \tag{1.4}$$

where p_i is the probability to be in a specific site, equal to $|\psi_i|^2$ for a quantum wave function. For a fully extended mode $PN \sim N$, while for a state occupying only one site $PN = 1$.

Another idea called Thouless curvature or Thouless conductance [3–5], is based on the idea that localized eigenmodes are almost not sensitive to boundary conditions. We apply a phase change ϕ across the boundary, (due to gauge invariance the specific spot is irrelevant), and check the resulting change in the eigenvalues. In an ordered system with extended modes, $\phi = \pi$ will cause an energy shift larger than the level spacing. Using perturbation theory on Kubo's equation [6], Thouless defined a conductance that is proportional to the diffusion:

$$\langle g_T \rangle \equiv \pi \frac{\left\langle \left| \frac{\partial^2 E^{(n)}}{\partial \phi^2} \right|_{\phi \to 0} \right| \right\rangle}{\Delta} \tag{1.5}$$

where Δ is the level spacing.

Because we have defined the diagonal by requiring each row and column to nullify, there always exists a special extended $\lambda = 0$ mode with all probabilities equal. Actually, in our $d \leq 2$ models, the localization length diverges as $\lambda \to 0$, So that while the states are localized by definition, in practice they may be very wide compared to the system length.

1.4 Modeling quantum diffusion with resistor networks

In a model described by a Hamiltonian

$$\mathcal{H} = \mathrm{diag} E_n + \epsilon V_{nm} \tag{1.6}$$

according to the first step of perturbation theory, for very short time the transition probability is:

$$p(n, n_0) \;=\; \left| \epsilon \left\langle n|V|n_0 \right\rangle t \right|^2 \;=\; \epsilon^2 t^2 \left| \langle n|V|n_0 \rangle \right|^2 \tag{1.7}$$

This suggests that for some short time scale, the ballistic behavior of the system might relate to the conductivity of the rate equation $G_{nm} = \left| \langle n|V|n_0 \rangle \right|^2$.

1.5 Heat conductance

One can take one of our suggested models, and couple each end to a different heat bath. In steady state, it is expected that the heat current will obey Fourier's law:

$$j = -\kappa \nabla T \tag{1.8}$$

Assuming κ does not change significantly with temperature, a given temperature difference δT over sample length L should yield:

$$j = \frac{\kappa \delta T}{L} \tag{1.9}$$

However, many one-dimensional models [7–10] exhibit sample size scaling of the form

$$j \propto L^{\alpha-1} \quad [\alpha > 0] \tag{1.10}$$

$$\kappa \propto L^{\alpha} \tag{1.11}$$

It is debated whether for $d = 1$ systems with momentum conservation, $\alpha = 1/3$,$\alpha = 2/5$ or neither [7, 11–13]. For several systems it has been shown that α depends on some tunable potential [14], and it also depends on the spectrum of the baths [8].

The total heat conductance is defined by

$$J = \int_0^\infty \rho(\lambda) g(\lambda) d\lambda \tag{1.12}$$

where $\rho(\omega)$ is the density of states, and $g(\lambda)$ is a transmission coefficient for a phonon at energy λ. $g(\lambda)$ is highly affected by the localization length of this mode, and one way to find it is via Thouless' curvature Equation 1.5. The high frequency eigenmodes are strongly localized, hence only the first part of the spectrum contributes to the heat flux. Based on this idea, the heat flux can be estimated [15, 16], by the number of wide modes.

1.6 Banded matrices spectrum

For wide bandwidth and uncorrelated matrix elements, the high eigenvalues should follow the Wigner semicircle law ($g(\lambda) = \frac{2}{\pi R^2}\sqrt{R^2 - \lambda^2}$) [17–19]. However, the low eigenvalues can still follow other rules, allowing for a transition between diffusion and subdiffusion.

Chapter 2

Objectives

The first two objectives have been the target of my MSc, and are covered in an article published at Physical Review E [20], and reprinted here in Appendix A. The other objectives will be pursued during my PhD research.

2.1 Diffusion or Subdiffusion in $2d$

For the stochastic random network, the question of diffusion in most $1d$ systems was analytically solved in [21]. The $2d$ case is, as far as we know, not yet analytically solved, and is much less clear. In [21] it is claimed that in low density systems subdiffusion of order $\sim log^d$ should occur. We wish to examine these networks through their spectral properties to find out if this is indeed the case. Our focus will be on low densities, and on checking whether there exists a transition between low densities and high densities.

Another aspect we wish to investigate is the influence of geometrical and topological features on the physics of the system, beyond the direct effect of changing the matrix elements statistics.

2.2 Banded sparse matrices

Between the $1d$ nearest neighbor network and the $2d$ network, lie the quasi $1d$ network, which allows transitions to further neighbors. The conductance of quasi-$1d$ banded sparse matrices was studied numerically in [22]. There, they generalized the *Variable-Range-Hopping* scheme

to treat matrices in the sparse regime, where (sparsity $\cdot$ bandwidth) $\ll 1$. However, in this work it is not clear what are the limits on either sparsity or bandwidth, and in particular where is the cross between the validity regime of VRH and that of SLRT. We will try to understand this issue analytically.

2.3 Models with relaxation

Up to now we have dealt with symmetric matrices only, but as presented in the introduction section 1.1, in general the transition rates may be assymetric. We wish to extend the methods used so far to develop a better estimation method for the transport in these assymetrical matrices.

2.4 Heat transport

Heat conduction by phonons is also affected by the localization properties of the model. If disorder scatters normal modes and induces diffusive energy transport, followed by normal heat conduction, then in accordance to Fourier's law, the heat current J depends inversely on the system size: $J \sim N^{-1}$. However, in recent studies **??** it was shown that $J \sim N^{-\alpha}$ with $\alpha \neq 1$ is sometimes the case for disordered $1d$ harmonic chains. We wish to investigate the validity of Fourier's law for quasi-$1d$ and higher dimensional disordered systems.

2.5 The spectral properties of Sinai diffusion in $1d$

In a symmetric $1d$ random rate system, there is regular diffusion if the harmonic average is bounded, i.e. if

$$\sum_n \frac{1}{w_n} < \infty \tag{2.1}$$

On the other hand, for an asymmetric system, an activation energy builds up, and a Sinai diffusion behavior is followed. The conductance is exponentially small in the length, and the spreading is anomalous. The difference between those two models is clearly highly significant. We wish to investigate the difference between the models, and the relation of this difference to the spectral properties of the model.

2.6 Sinai diffusion in $2d$

We shall inspect the spectral properties, and spreading behavior of a $2d$ asymmetric system. The $2d$ case is much different than the $1d$ case, because particles can circumvent barriers. Interestingly, a nearest neighbor lattice can be constructed to present the same long time spreading as the $1d$ lattice [23]. The question is whether having nearest neighbor links only is a necessary condition for this behavior, and how does this relate to the spectral properties of the $2d$ system.

2.7 Quantum spreading

Up to now, we have concentrated on Markovian networks, dealing with the probabilities without phases. We will try to generalize the work to solve Hamiltonian matrices of the same genre. With a coherent Hamiltonian, we expect suppression of the diffusion due to Anderson localization. However there may be transient diffusion, which would persist for infinite time in the presence of dephasing.

We intend to examine the applicability of the resistor network picture for the calculation of the diffusion coefficient in these quantum networks, beginning with a simple model described by a real symmetric Hamiltonian:

$$\mathcal{H}_{nm} = \text{random}[\pm]\text{e}^{-\text{random}[x]} \qquad 0 < |n-m| \leq b \tag{2.2}$$

Where the parameter x is distributed uniformly $x \in [0, \sigma]$.

2.8 The charge carrier discreteness

Our work so far considered probability rate equations and single-particle Hamiltonians, which are valid for a single particle in the network. Having many non interacting particles is equivalent to having many realizations of a single particle, leaving the picture intact. However, if we have multiple *interacting* particles in the network, additional factors may contribute. For example, a single occupancy rule (i.e. each site may have up to one particle) may cause Fermi blocking. Another issue is that the single particle behavior might differ from the bulk behavior, e.g. it could be sub-diffusive while the bulk spreading is diffusive [24, 25].

Part II

Completed Work and Preliminary Analysis

Chapter 3

Completed Work

This work was published at Physical Review E [20], and reprinted here in Appendix A. In the following sections we will provide an overview of the main results.

3.1 Regular diffusion in the $2d$ sparse network

We studied models with a rate equation of the type $w_{ij} = w_0 \exp -r_{ij}/\xi$ (see section II of the attached article). In particular, we have mapped the $d = 1$ model to known results of the transport and survival [21], and compared this with our numerics.

The $d = 2$ case was studied using RG techniques in [21, 26], where it was suggested that anomalous diffusion takes place for sparse configurations. However, our analysis indicates that for any amount of sparsity, the diffusion is regular ($S(t) \sim (2d)(Dt)$).

3.2 The effective range hopping procedure

Feeling unsatisfied with the linear expression for the diffusion in sparse systems, we set off for a better diffusion approximation.

The basic idea behind *ERH* (effective range hopping) is that in the linear expression, nearby sites with $r \ll 1$ (and therefore $w \gg 1$) are over represented in the diffusion coefficient calculation. While the transition to these sites is indeed high, the distance covered is not enough to form a percolating cluster. Therefore, we use a threshold based on percolation theory and flat-down the rates higher then this threshold.

Using the *ERH* procedure we have calculated the diffusion for several models.

For the $d = 2$ ordered lattice with nearest neighbor random hopping:

$$D_{\rm ERH} = \left[\frac{1}{2}w_c + \frac{1}{2}\int_0^{w_c} w\tilde{f}(w)dw\right] r_0^2 \tag{3.1}$$

In absence of the disorder (i.e. all the rates are equal), the known result $D = w_0 r_0^2$ is restored.

For the degenerate hopping model,

$$D_{\rm ERH} = {\rm EXP}_{d+2}\left(\frac{1}{s_c}\right)\ {\rm e}^{-1/s_c}\ D_{\rm linear} \tag{3.2}$$

For the Mott Hopping model,

$$D_{\rm ERH} = {\rm EXP}_{d+3}\left(\epsilon_c\right)\ {\rm e}^{-\epsilon_c}\ D_{\rm linear} \tag{3.3}$$

For the flat-profile banded $1d$ model,

$$D_{\rm ERH} \quad = \quad \frac{1}{\sigma}\left[\left(1 + \frac{n_c}{2b}\sigma\right){\rm e}^{-\frac{n_c}{2b}\sigma} - {\rm e}^{-2\sigma}\right]\ \tilde{b}w_0 \tag{3.4}$$

Chapter 4

Preliminary analysis

4.1 The quasi one dimensional rate equation

The quasi one dimensional system, is a one dimensional system with a bandwidth greater than 1 (going beyond nearest neighbors). We continue our theme by studying the survival and transport properties in those systems, specifically in sparse configurations.

In recent studies [16] an interesting structure of PN (participation number) was observed in a similar model. In this model, N equal masses are connected by springs up to a bandwidth b. In addition to these springs, there are "pinning" springs from each mass to its initial position, with strength ϵ_n, as described by the classical Hamiltonian:

$$\mathcal{H} = \sum_n \left(\frac{p_n^2}{2m} + \epsilon_n \frac{x_n^2}{2} + \frac{1}{2} \sum_j \frac{1}{2} k_{nj} (x_n - x_j)^2 \right) \tag{4.1}$$

$$= \sum_n \frac{p_n^2}{2m} + \frac{1}{2} \vec{x}^{\intercal} K \vec{x} \tag{4.2}$$

$$K_{nm} = \begin{cases} \sum_{l \neq n} k_{ln} + \epsilon_n & \text{if} \quad n = m \\ -k_{nm} & \text{if} \quad n \neq m \end{cases} \tag{4.3}$$

$$\vec{x} = (x_1, x_2, \ldots, x_N) \tag{4.4}$$

The disorder is introduced by randomized k_{ij} and ϵ_n.

As can be seen in **??**, for the low eigenvalues, instead of the expected large PN, we have some decrease. After that, follows a period of large PN, followed by another segment with somewhat smaller PN. Another quantity we calculated is the Thouless conductance (see

section 1.3), which we expect to correlate with PN. Disregarding major numerical issues, the correlation seems to hold, see Figure 4.1d.

4.2 The quasi one dimensional Hamiltonian

In this section the numerical work was done by our collaborators, Eli Halperin and Tsampikos Kottos of Wesleyan university.

In this model , described in **??**, initial analysis of the numerical results reveals that the sparsity affects the diffusion coefficient. We see that as the system becomes more sparse, the diffusion coefficient is suppressed. As might be expected, the lower bandwidth ensembles are more susceptible, as the system is more vulnerable to disconnections.

Our first question was whether our rate equation analysis might hold also for the quantum case, because in first order perturbation theory, the transition probability p_{nm} is proportional to $|\langle n|\mathcal{H}|m\rangle|^2$. Naively using our previously obtained suppression factor $g_s = \frac{D_{ERH}}{D_{\text{linear}}}$, did not prove to be sufficient, as can be seen in Figure 4.3.

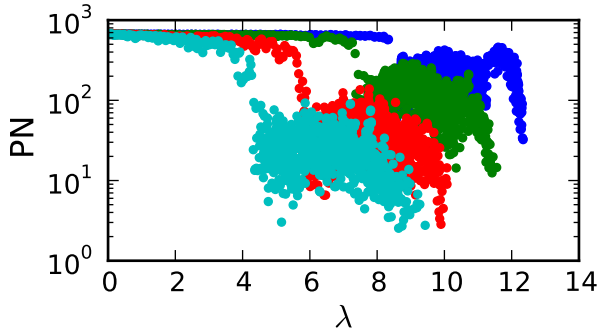

(a) Low sparsity, without diagonal disorder. $\sigma = 0.1$ in blue, 0.2 in green, 0.3 in red and 0.4 in cyan.

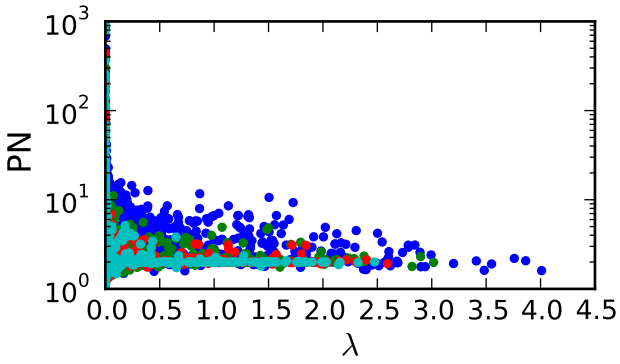

(b) High sparsity, without diagonal disorder. $\sigma = 1$ in blue, 2 in green, 3 in red and 4 in cyan.

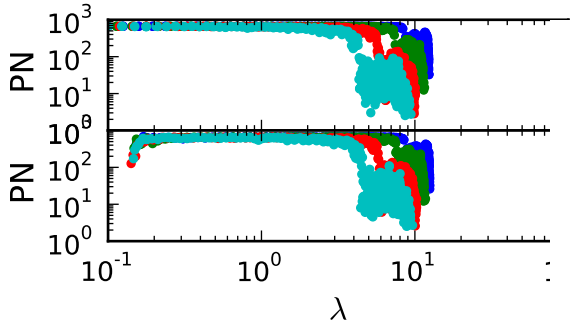

(c) Above- without diagonal disorder
Below - with diagonal disorder
$\sigma = 0.1$ in blue, 0.2 in green, 0.3 in red and 0.4 in cyan.

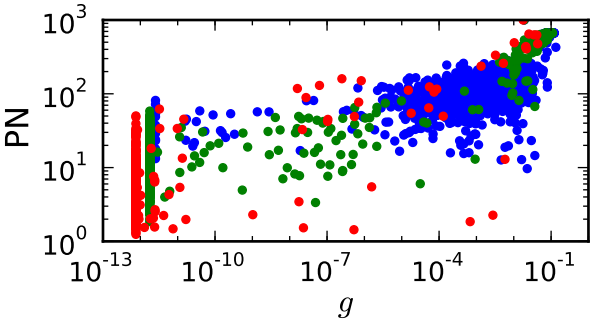

(d) PN as a function of g. $\sigma = 0.2$ in blue, 1 in green, 10 in red.

Figure 4.1: (abc) - **PN** as a function of λ. For all the plots $N = 1000$ and $b = 5$. The off diagonal elements are $w_{ij} = \mathrm{e}^{-\epsilon} \quad \epsilon \in \text{uniform}[0, 2\sigma]$. For (cb), the diagonal elements are $w_{ii} = -\sum_j w_{ij}$, while in the lower plot of (c) we added a uniform disordered parameter $x \quad \in \text{uniform}[0, 0.3]$ to the diagonal. Comparing the two plots in c, our initial numerical analysis shows that the low-eigenvalue decrease is caused by the diagonal disorder. This disorder removes the one special $\lambda = 0$ eigenmode, and decreases the PN of several other modes. In b, we see that once we use a much wider distribution of off diagonal elements, i.e. increase the *sparsity*, the two segment structure disappears. (d) - comparing the Thouless conductance g with the participation number. The presented points do seem to be correlated, but due to numerical issues, many values of g are below the precision limit (seen as a vertical line in the plot), up to 936 from 1000 for $\sigma = 10$. In our numeric algorithm, the eigenvalue precision is relative to the highest eigenvalue. For wide distributions of eigenvalues, that means that the numerical precision of the low eigenvalues is poor, and the uncertainty is larger than the phase induced shift.

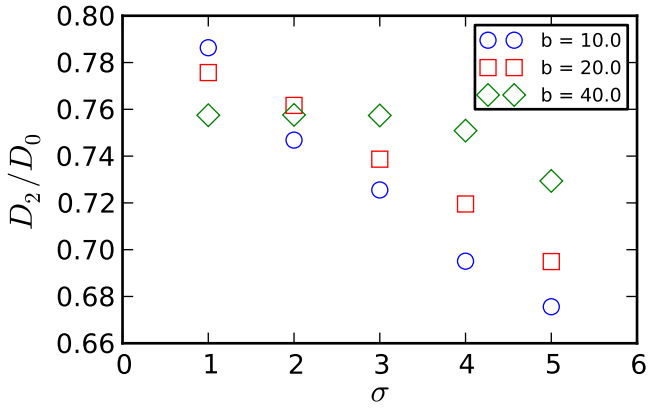

Figure 4.2: The transient diffusion coefficient for quantum spreading in a banded sparse network. The ratio D/D_0 between the numerical diffusion coefficient and the expected value decreases as σ increases. The effect is stronger for low bandwidth.

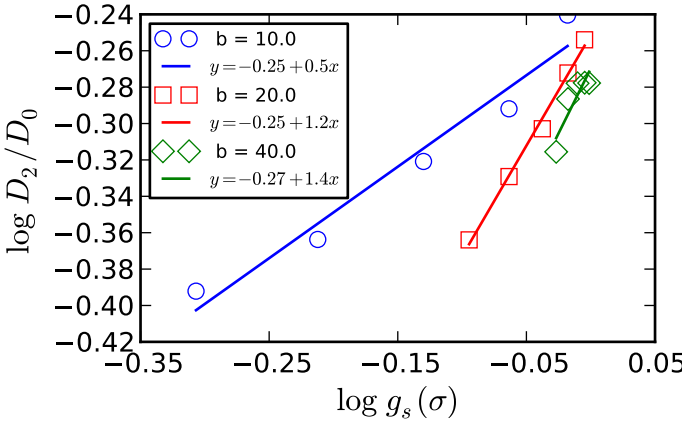

Figure 4.3: Scaled D vs g_s.

Part III

Appendix

Appendix A

Published Paper

Diffusion in sparse networks: Linear to semilinear crossover

Yaron de Leeuw and Doron Cohen
Department of Physics, Ben Gurion University of the Negev, Beer Sheva 84105, Israel
(Received 12 June 2012; revised manuscript received 27 September 2012; published 19 November 2012)

We consider random networks whose dynamics is described by a rate equation, with transition rates w_{nm} that form a symmetric matrix. The long time evolution of the system is characterized by a diffusion coefficient D. In one dimension it is well known that D can display an abrupt percolation-like transition from diffusion ($D > 0$) to subdiffusion ($D = 0$). A question arises whether such a transition happens in higher dimensions. Numerically D can be evaluated using a resistor network calculation, or optionally it can be deduced from the spectral properties of the system. Contrary to a recent expectation that is based on a renormalization-group analysis, we deduce that D is finite, suggest an "effective-range-hopping" procedure to evaluate it, and contrast the results with the linear estimate. The same approach is useful in the analysis of networks that are described by quasi-one-dimensional sparse banded matrices.

DOI: 10.1103/PhysRevE.86.051120 PACS number(s): 05.40.−a, 02.10.Yn, 63.50.−x, 71.23.Cq

I. INTRODUCTION

The study of network systems is of interest in the diverse fields of mathematics, physics, and computer and life sciences. Commonly a network is described by a symmetric matrix that consists of real non-negative elements, e.g., the adjacency matrix or the link probability matrix, that have unique spectral properties [1,2]. Physically motivated, in this work we consider d-dimensional network systems, whose dynamics is described by a rate equation

$$\frac{dp_n}{dt} = \sum_m w_{nm}\, p_m. \tag{1}$$

The off-diagonal elements of $\boldsymbol{w}$ are the transition rates, while the diagonal elements are the decay rates

$$w_{nn} = -\gamma_n, \quad \gamma_n \equiv \sum_{m(\neq n)} w_{mn}. \tag{2}$$

We assume a symmetric matrix and write schematically

$$\boldsymbol{w} = \text{matrix}\{w_{nm}\}. \tag{3}$$

In some sense, one can regard $\boldsymbol{w}$ as a discrete Laplacian that is associated with the network. Clearly the physical problem is related to the study of random walk in a disordered environment [3–5].

For presentation purposes we regard the nodes of the network as *sites*, each having a location x_n. By construction, we assume that the transition rates w_{nm} are given by the expression $w_0 e^{-\epsilon_{nm}} B(x_n - x_m)$, where $B(r)$ describes the systematic dependence of the coupling on the distance between the sites, and ϵ is a random variable that might represent, say, the activation energy that is required to make a transition. Consequently the network is characterized by two functions:

$$w(r,\epsilon) \equiv w_0\, e^{-\epsilon}\, B(r), \tag{4}$$

$$\rho(r,\epsilon) \equiv \text{local density of sites}. \tag{5}$$

The latter is defined as the density of sites in (r,ϵ) space, relative to some initial site. Obviously the functional dependence of this density on r is affected by the dimensionality of the network.

Sparsity. Our interest is focused on "sparse" networks. This means that the transition rates between neighboring sites are log-wide distributed as in glassy systems. These rates span several orders of magnitudes as determined by the dispersion of r or by the dispersion of ϵ. In particular (but not exclusively) we are interested in a random site model where the rates depend exponentially on the distance between randomly distributed sites, namely, $B(r) = \exp(-r/\xi)$. In this particular case one can characterize the sparsity by the parameter

$$s = \xi/r_0, \tag{6}$$

where r_0 is the average distance between neighboring sites. We refer to such networks as "sparse" if $s \ll 1$.

Sparsity vs percolation. The problem that we consider is a variant of the percolation problem [6]. Instead of considering a bimodal distribution ("zeros" and "ones") we consider a log-wide distribution of rates [7], for which the median is much smaller than the mean value. We call such a network sparse because the large elements constitute a minority.

Sparsity vs disorder. While the standard percolation problem can be regarded as the outcome of extreme sparsity, the latter can be regarded as arising from an extreme disorder. Accordingly, the model that we are considering is a close relative of the Anderson localization problem, and therefore we shall dedicate some discussion to clarify the relation.

Physical context. The model that we address is related and motivated by various physical problems, for example, phonon propagation in disordered solids [8–10], Mott hopping conductance [7,11–15], transport in oil reservoirs [16,17], conductance of ballistic rings [18], and energy absorption by trapped atoms [19]. Optionally these models can be fabricated by combining oscillators, say, mechanical springs or electrical resistor-capacitor elements. In all these examples the issue is to understand how the *transport* is affected by the *sparsity* of a network. If the rates are induced by a driving source, this issue can be phrased as going *beyond* the familiar framework of linear response theory, as explained below.

Diffusion and subdiffusion. Our interest is focused on the diffusion coefficient D that characterizes the long time dynamics of a spreading distribution. The simplest way to define it, as in standard textbooks, is via the variance

$S(t) \equiv \langle r^2 \rangle_t$. Namely,

$$D \equiv (2d)^{-1} \lim_{t\to\infty} \frac{S(t)}{t}. \tag{7}$$

Optionally it can be defined or deduced from the decay of the survival probability $\mathcal{P}(t) \sim (Dt)^{-d/2}$. Hence it is related to the spectral properties of the transition rate matrix.

In the $d = 1$ case, it is well known [20] that D can display an abrupt percolation-like transition from diffusive ($D > 0$) to subdiffusive ($D = 0$) behavior, as the sparsity parameter drops below the critical value $s_{\rm cr} = 1$. Similar anomalies are found for fractal structures with $d < 2$, also known as "random walk on percolating clusters," see [21–25]. A question arises as to whether such a transition might happen in higher dimensions.

In [10] the spectral properties in the $d = 2$ case were investigated: on the basis of the renormalization group (RG) procedure it was deduced that $\mathcal{P}(t)$ decays in a logarithmic way, indicating anomalous (sub) diffusion. In the present work we shall introduce a different approach that implies, contrary to the simple RG treatment, that in spite of the sparsity, the long time dynamics is in fact diffusive rather than subdiffusive.

Resistor network picture. One can regard the p_n in Eq. (1) as the charge in site n; each site is assumed to have unit capacitance; hence $p_n - p_m$ is the potential difference, and $w_{nm}(p_m - p_n)$ is the current from m to n. Accordingly Eq. (1) can be regarded as the Kirchhoff equation of the circuit. While calculating D it is illuminating to exploit the implied formal analogy with a resistor network calculation [12,14,18,26]. Namely, regarding w_{nm} as connectors, it follows that D is formally like conductivity. It follows that $D[\boldsymbol{w}]$ is in general a *semilinear* function:

$$D[\lambda \boldsymbol{w}] = \lambda D[\boldsymbol{w}], \tag{8}$$

$$D[\boldsymbol{w}^a + \boldsymbol{w}^b] > D[\boldsymbol{w}^a] + D[\boldsymbol{w}^b]. \tag{9}$$

If the rates are induced by a driving source, the above super additivity implies that the analysis should go *beyond* the familiar framework of linear-response theory [27].

In this work we obtain an improved estimate for D that we call effective range hopping (ERH). Using this approach we show that in the $d = 2$ case, as s becomes small, the functional $D[\boldsymbol{w}]$ exhibits a smooth crossover from linear behavior to semilinear VRH-type dependence. Our approach is inspired by the resistor network picture of [7,12–19,27], and leads in the appropriate limit to the well-known Mott's variable range hopping (VRH) estimate for D.

Outline. We first describe some known results and some additional numerical results for the spectral properties of $d = 1$ and $d = 2$ networks and for the dependence of D on the sparsity. Then we show that an ERH procedure is useful in describing the crossover from the linear regime (no sparsity) to the semilinear regime. In the latter regime a resistor network approach is essential, and the percolation threshold manifests itself in the calculation. Finally we demonstrate that the same ERH procedure can be applied in the case of a quasi-one-dimensional network that is described by a sparse banded random matrix. The latter is of relevance to previous studies of energy absorption by a weakly chaotic system [27]. We conclude with a discussion and a short summary.

II. RANDOM SITE HOPPING MODEL

Consider a network that consists of sites that are distributed in space, locations x_n. With each bond nm we associate an activation energy $\epsilon_{nm} > 0$, and assume

$$w_{nm} = w_0\, e^{-\epsilon_{nm}}\, e^{-|x_n - x_m|/\xi}. \tag{10}$$

Accordingly we have the identification

$$B(r) = e^{-r/\xi}. \tag{11}$$

We note that in the traditional formulation of the Mott problem the activation energies are not due to some barriers, but are determined by the on-site binding energies, namely, $\epsilon_{nm} = |\varepsilon_n - \varepsilon_m|/T$, where T is the temperature. In this paper we treat the ϵ_{nm} as an uncorrelated random variable.

The density of sites relative to some initial site is characterized by a joint distribution function

$$\rho(r,\epsilon)dr\, d\epsilon = \frac{\Omega_d\, r^{d-1} dr}{r_0^d}\, f(\epsilon)d\epsilon, \quad \Omega_d = 2,2\pi,4\pi. \tag{12}$$

We distinguish between the Mott hopping model and the degenerate hopping model. Namely,

$$f(\epsilon) = 1 \quad \text{Mott hopping model,} \tag{13}$$

$$f(\epsilon) = \delta(\epsilon) \quad \text{Degenerate hopping model.} \tag{14}$$

The normalization of $f(\epsilon)$ as defined above fixes the value of the constant r_0^d, which we regard as the "unit cell." In the numerics we set the units of distance such that $r_0 = 1$.

In the traditional formulation of the Mott problem it is assumed that mean level spacing within ξ^d is Δ_ξ, such that the number of accessible sites is $(d\varepsilon/\Delta_\xi)(d^3r/\xi^d)$. By the convention of Eq. (12) this implies that the unit cell dimension is temperature dependent

$$r_0^d = \left(\frac{\Delta_\xi}{T}\right)\xi^d \quad \text{[for Mott model].} \tag{15}$$

We reemphasize that the number of sites per unit volume in the Mott problem is infinite, but effectively only $\sim T/\Delta_\xi$ sites are accessible within ξ^d per attempted transition. It is convenient to characterize a random site model by a sparsity parameter that is defined as in Eq. (6). Accordingly

$$s \equiv \frac{\xi}{r_0} = \left(\frac{T}{\Delta_\xi}\right)^{1/d} \quad \text{[for Mott model].} \tag{16}$$

We refer to a network as sparse if $s \ll 1$.

The lattice model with near-neighbor (n.n.) transitions is one of the most popular models in statistical mechanics: in particular the random walk problem on a lattice is a standard textbook example. If the rates are generated from a log-wide distribution, it can be regarded as a variant of the random site hopping model. For details see Appendix A. In particular we note that the $d = 1$ version is formally equivalent: it does not matter whether the distribution of w is due to random distances r or due to random activation energies ϵ.

Finally we note that a quasi-one-dimensional version of the random site model arises in the study of energy absorption as explained in Appendix B, and later addressed in Sec. XI.

III. CHARACTERIZATION OF TRANSPORT

The long time dynamics that takes place on the network is characterized by the spreading $S(t)$ and by the survival probability $\mathcal{P}(t)$. If the system is diffusive, these functions have the following functional form:

$$S(t) = \langle r^2 \rangle_t \sim (2d)Dt, \tag{17}$$

$$\mathcal{P}(t) \sim \frac{r_0^d}{(4\pi\, Dt)^{d/2}}. \tag{18}$$

See Appendix C for details. The diffusion coefficient D appears here in consistency with its definition in Eq. (7). We note that in the case of subdiffusion

$$S(t) \propto t^{\alpha}, \quad [\alpha < 1], \tag{19}$$

which implies by Eq. (7) that $D = 0$.

The spectrum of the matrix $\boldsymbol{w}$ consists of the trivial eigenvalue $\lambda_0 = 0$ that is associated with a uniform distribution, and a set of negative numbers $-\lambda_k$ that describe the decaying modes. The spectral function $\mathcal{N}(\lambda)$ counts the number of eigenvalues up to the value λ. We normalize it per site such that $\mathcal{N}(\infty) = 1$. The associated density of eigenvalues $g(\lambda)$ is related to $\mathcal{P}(t)$ by a Laplace transform. See Appendix C for details. It follows that in the case of a diffusive system

$$\mathcal{N}(\lambda) = \int^{\lambda} g(\lambda) d\lambda \sim \left(\frac{r_0}{2\pi}\right)^d \left[\frac{\lambda}{D}\right]^{d/2}. \tag{20}$$

In Appendix D we clarify that this expression agrees with the Debye law. Accordingly the calculation of D parallels the calculation of the speed of sound c in the Debye model.

Regarded as a transport coefficient D relates the probability current to the density gradient. This is known as Fick's law. From the discussion in the Introduction it follows that D is like the *conductivity* of a resistor network, which relates the electrical current to the voltage difference. Some further details on the practical calculation of the conductivity are presented in Appendix E. On the basis of this analogy it should be clear that $D[\boldsymbol{w}]$ is in general a *semilinear* function of the rates, see Eq. (9).

IV. EXACT AND NUMERICAL RESULTS FOR THE $d = 1$ LATTICE MODEL

In the case of a $d = 1$ lattice model with n.n. transitions it is natural to use the notation $w_n = w_{n,n-1}$. Pointing out the analogy with adding connectors in series, the expression for D is

$$D = \left(\frac{1}{N}\sum_n \frac{1}{w_n}\right)^{-1} = \frac{s-1}{s}\, w_0 [s > 1]. \tag{21}$$

The calculation that leads to the last equality has been done with the distribution of Eq. (A2), where $s \equiv \xi/r_0$. Note that we have here a serial addition of resistors $R = \sum_n R_n$, where $R_n = 1/w_n$. For $s < 1$ the distribution of each R_n is dominated by the large values, hence $R = \infty$. On the other extreme for $s > 1$ the distribution of the R_n has finite first and second moments, and accordingly the result for R becomes self-averaging, as implied by the central limit theorem. This means the D is well defined only for $s > 2$. For $1 < s < 2$ the result for the average R is finite but not self-averaging.

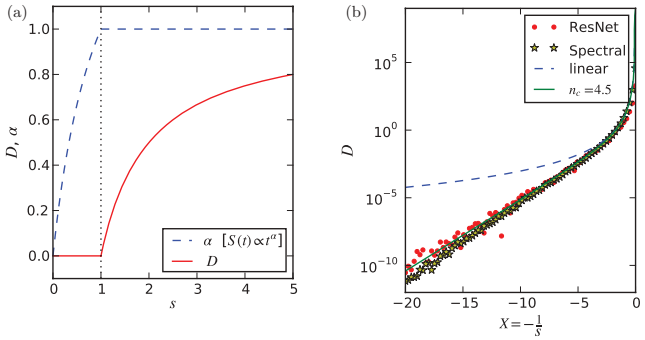

FIG. 1. (Color online) Spreading in (a) the $d = 1$ lattice model and (b) the $d = 2$ degenerate random site model. Panel (a) is based on known exact results. Its dashed blue line is the power α of the spreading, showing a subdiffusive regime for $s < 1$, and a diffusive regime for $s > 1$. Its solid red line is the diffusion coefficient D, which is zero in the subdiffusive regime. Panel (b) displays numerical results that refer to a network that consists of $N = 2000$ sites randomly scattered over a square with periodic boundary conditions. The vertical axis is the diffusion coefficient D in a logarithmic scale, while the horizontal axis is $X = -1/s$. The numerical red dots are based on a resistor network calculation (see Appendix E), while the stars are extracted from the spectral analysis (see Fig. 2). The dashed line is the linear estimate (corresponds to $n_c = 0$), while the solid line is the ERH estimate with $n_c = 4.5$. One observes that the ERH calculation describes very well the departure from the linear prediction.

The dependence of D on s is illustrated in Fig. 1(a). In the subdiffusive regime ($s < 1$), where the result for the diffusion coefficient is $D = 0$, the dynamics becomes subdiffusive. The explicit results for the survival probability and for the spreading are known [20]:

$$S(t) \sim t^{2s/(1+s)}, \tag{22}$$

$$\mathcal{P}(t) \sim t^{-s/(1+s)}, \tag{23}$$

and the associated spectral function is

$$\mathcal{N}(\lambda) \sim \lambda^{s/(1+s)}. \tag{24}$$

The numerical demonstration of the latter expectation is displayed in Fig. 2 (left upper panel). We clearly see that for $s < 1$ the asymptotic slope corresponds to subdiffusion, while for $s > 1$ it corresponds to diffusion.

V. NUMERICAL RESULTS FOR THE $d = 2$ RANDOM SITE MODEL

Results for the spectral counting function of the degenerate $d = 2$ random site model are presented in Fig. 2 (right upper panel). We also display there (in the lower panel) the participation number (PN) for each eigenstate. The PN of an eigenstate that corresponds to an eigenvalue λ_k is conventionally defined as

$$\mathrm{PN} \equiv \left[\sum_n |\langle n|\lambda_k\rangle|^4\right]^{-1}. \tag{25}$$

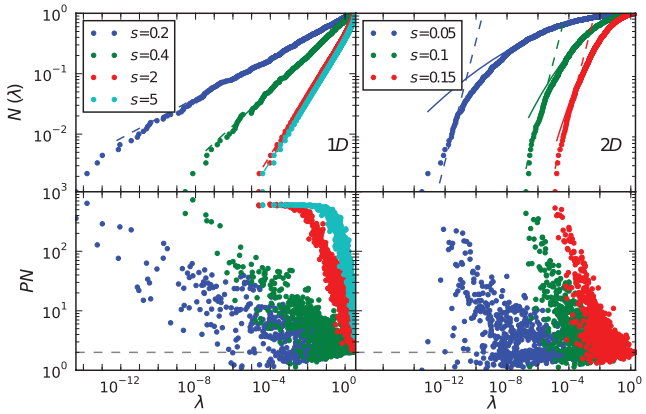

FIG. 2. (Color online) Cumulative eigenvalue distributions $\mathcal{N}(\lambda)$ for the $d = 1$ (1D) and for the $d = 2$ (2D) models of Fig. 1, and the respective PN of the eigenstates (lower panels). Several representative values of s are considered. The dots are determined via numerical diagonalization of $N \times N$ matrices, each representing a network that consists of $N = 1000$ sites randomly scattered over a square with periodic boundary conditions. There is a striking difference between the $d = 1$ and the $d = 2$ cases. For $d = 1$, the log-log slope of $\mathcal{N}(\lambda)$, see dashed lines, is less than $d/2$ for sparse networks ($s < 1$), meaning that we have subdiffusion. In the $d = 2$ case the small-λ log-log slope is always $d/2$, which corresponds to normal diffusion. The solid lines in the upper 2D plot are according to the RG analysis of [10], namely, Eq. (26). The horizontal dashed line in the lower panels indicates the special value PN= 2 that corresponds to dimer formation.

As expected from the study of localization in a disordered elastic medium [28], the PN becomes larger in the limit $\lambda \to 0$, without apparent indication for a mobility threshold.

Assuming localized modes that are conceived via dimerization of neighboring sites, $\mathcal{N}(\lambda)$ should equal the probability $\exp[-\mathsf{V}(r)/r_0^d]$ not to have any neighboring site within the volume $\mathsf{V}(r)$ of the sphere $2w_0 \exp(-r/\xi) > \lambda$. The RG analysis of [10] refines this naive expectation, adding a factor of 2 in the exponent, leading to

$$\mathcal{N}(\lambda) = \exp\left\{ -\frac{\Omega_d}{2d}\left[-s \ln\left(\frac{\lambda}{2w_0}\right)\right]^d \right\}, \tag{26}$$

where $s \equiv \xi/r_0$. This expectation is represented in Fig. 2 (right upper panel) by solid lines. We see that it fails to capture the small λ regime, where the distribution corresponds to diffusive behavior.

Extracting D via fitting to Eq. (20) we get Fig. 1(b). We see that in the $d = 2$ model *there is no abrupt crossover to subdiffusion*. We therefore would like to find a way to calculate D, and hence to have the way to determine the small λ asymptotics.

Note added. One should conclude that the RG of Ref. [10] applies only to the analysis of the high frequency response, while our interest is focused in the low frequency (direct current) analysis. The crossover between the two regimes is implied. For more details in this direction see a followup work [29] that confirms our physical picture and demonstrates numerically the implied crossover.

VI. LINEAR AND ERH ESTIMATES FOR THE DIFFUSION COEFFICIENT

The standard way to calculate diffusion in a $d = 1$ random walk problem is to inspect the transient growth of the variance $\mathrm{Var}(n) = 2Dt$. In the stochastic context, if we start at site n we have $\mathrm{Var}(n) = \sum_{n'} p_{n'}(n'-n)^2$, with $p_{n'} = w_{n'n}t$, hence

$$D_n = \frac{1}{2}\sum_{n'}(n'-n)^2\, w_{n'n}. \tag{27}$$

The generalization to more than one dimension is straightforward. Averaging the transient expression over the starting point we get the result

$$D_{\mathrm{linear}} = \frac{1}{2d}\iint w(r,\epsilon) r^2 \rho(r,\epsilon) d\epsilon\, dr. \tag{28}$$

This expression is strictly linear. It describes correctly the average transient spreading. In the absence of disorder we can trust it for arbitrary long time. But if we have a disordered or sparse network, the possibility for transport is related to the theory of percolation [7,13,14]. We are therefore motivated to introduce an approximation scheme that takes the percolation aspect into account. We shall refer to this scheme as effective range hopping (ERH) because it is a variation on the well-known VRH procedure.

Inspired by [7,13,14] we look for the threshold w_c that is required for percolation. In the ERH scheme we suggest using the following equation for its determination:

$$\iint_{w(r,\epsilon)>w_c} \rho(r,\epsilon) dr\, d\epsilon = n_c. \tag{29}$$

Here n_c is the effective coordination number that is required for getting a connected sequences of transitions. For a $d = 2$ square lattice model it is reasonable to set $n_c = 2$, reflecting the idea of forming a simple chain of transitions. Rephrased differently the requirement is to have an average of 50% connecting bonds per site. For a $d = 2$ random site model one should be familiar with the problem of percolation in a system that consists of randomly distributed discs. The effective coordination number that is required for getting percolation in such a model is $n_c = 4.5$, as found in [30], and further discussed in Sec. IV A 1 of [31].

The second step in the ERH scheme is to form an effective network whose sparse elements are suppressed to the threshold value. Then it is possible to use the linear formula Eq. (28). Hence we get

$$D_{\mathrm{ERH}} = \frac{1}{2d}\iint \min\{w(r,\epsilon), w_c\}\, r^2\, \rho(r,\epsilon)\, d\epsilon\, dr. \tag{30}$$

This expression, as required, is semilinear rather than linear. It looks like the linear estimate of Eq. (28), but it involves a network with w_{nm} that are equal or smaller to the original values. The "suppressed" connectors are those that are too sparse to form percolating trajectories.

VII. VARIABLE RANGE HOPPING ESTIMATE

The ERH is similar to the generalized VRH procedure that we have used in previous publications [18,19]. The traditional VRH is based on the idea of associating an energy cost $\varepsilon(r)$ to

a jump that has range r. Namely,

$$\varepsilon(r) \sim \left[\frac{\Omega_d}{d} r^d\right]^{-1} \Delta_0, \tag{31}$$

corresponding to the average level spacing of the sites within a range r. In our notation, $\epsilon(r) \equiv \varepsilon(r)/T$. For the general network models that we consider here, the relation between ϵ and r is determined through the equation

$$\int_0^{\epsilon}\int_0^{r} \rho(r',\epsilon')dr'\,d\epsilon' = n^*, \tag{32}$$

where n^* is of order unity. In fact we shall deduce later, in Sec. X, that for consistency with the ERH estimate this value should be $n^* = n_c/d$. With the substitution of Eq. (12) the tradeoff equation can be written as

$$\Omega_d\left(\frac{r}{r_0}\right)^d F(\epsilon) = n_c, \tag{33}$$

where $F(\epsilon)$ is the cumulative distribution function that corresponds to the density $f(\epsilon)$. In the Mott problem $F(\epsilon) = \epsilon$, and Eq. (31) is recovered. In words, Eq. (32) asks what is the ϵ window that is required in order to guarantee that the particle will be able to find with probability of order unity an accessible site within a range r. Larger jumps allow smaller cost. Then we estimate D as follows:

$$D_{\rm VRH} \sim w^*(r^*)^2, \tag{34}$$

where r^* is the optimal range that maximizes $w(r,\epsilon(r))$, with associated energy cost $\epsilon^* = \epsilon(r^*)$, and effective transition rate $w^* = w(r^*,\epsilon^*)$. See Fig. 3 for illustration.

The VRH estimate, unlike the ERH, does not interpolate with the linear regime. It can be used to estimate D only if the system is very sparse ($s \ll 1$). It can be regarded as an asymptotic evaluation of the ERH integral: it assumes that the hopping is dominated by the vicinity of the optimal point (r^*,ϵ^*). Accordingly, VRH-to-ERH consistency requires

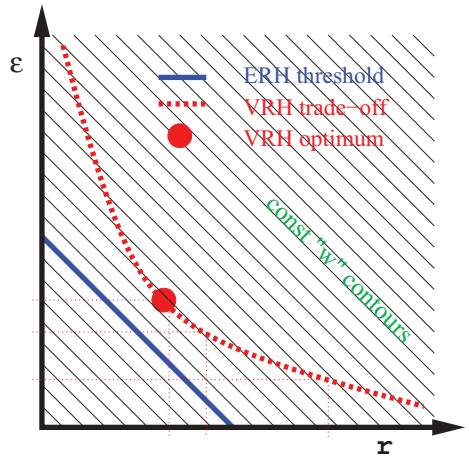

FIG. 3. (Color online) Comparing VRH with the ERH procedure. The solid blue line that corresponds to the ERH threshold w_c encloses an "area" that corresponds to n_c. The VRH tradeoff is represented by the dashed red line. The VRH optimum is represented by the thick red dot. The VRH-to-ERH consistency requirement [Eq. (46)] is to have the VRH optimum sitting on the solid blue line.

the identification $w^* = w_c$. However, using known results from percolation theory, one possibly can further refine the determination of the optimal value w^*. Namely, a somewhat smaller value than the threshold value w_c might allow a better connectivity. As s becomes very small, the effective range δw in the ERH integral, which contains the dominant contribution, becomes very small compared with $w_c - w^*$, and one should be worried about the implied (subdominant) correction. This speculative crossover is beyond the scope of the present study, and possibly very hard to detect numerically. A useful analogy here is with the crossover from "mean-field" to "critical" behavior in the theory of phase transition, as implied by the Ginzburg criterion.

VIII. ERH CALCULATION FOR THE $d = 2$ LATTICE MODEL

The $d = 2$ lattice model, as defined in Appendix A, is the simplest and most common example for studies of percolation and percolation-related problems. We substitute into Eq. (29) the effective density Eq. (A3) with the coordination number $c_L = 4$, and deduce that w_c is merely the *median* value of the n.n. transition rates. The ERH calculation using Eq. (30) with Eq. (A3) requires a simple $f(\epsilon)d\epsilon$ integration, which can be rewritten as a $\tilde{f}(w)dw$ integral. This integral is the sum of $w > w_c$ and $w < w_c$ contributions, namely,

$$D_{\rm ERH} = \left[\frac{1}{2}w_c + \frac{1}{2}\int_0^{w_c} w\tilde{f}(w)dw\right] r_0^2. \tag{35}$$

Note that the first term in the square brackets originates from the $w > w_c$ contribution. Note also that the result is $D = w_c r_0^2$ for a delta distribution, i.e., in the absence of disorder.

IX. ERH CALCULATION FOR THE DEGENERATE HOPPING MODEL

We now turn to the calculation of the ERH estimate for the degenerate hopping model. The ERH threshold can be written as $w_c = w_0 \exp(-r_c/\xi)$, where r_c is determined through Eq. (29), which takes the form

$$\int_0^{r_c} \frac{\Omega_d r^{d-1} dr}{r_0^2} = n_c, \tag{36}$$

leading to

$$w_c = w_0 \exp\left(-\frac{r_c}{\xi}\right), \tag{37}$$

$$r_c \equiv \left(\frac{d}{\Omega_c} n_c\right)^{1/d} r_0. \tag{38}$$

The calculation of the ERH integral of Eq. (30) is detailed in Appendix F. We note that the linear approximation of Eq. (28) is formally obtained by setting $r_c = 0$, leading to

$$D_{\rm linear} = \frac{(d+1)!\,\Omega_d}{2d} s^{d+2} w_0 r_0^2. \tag{39}$$

Then it is possible to write the result of the ERH integral as

$$D_{\rm ERH} = {\rm EXP}_{d+2}\left(\frac{1}{s_c}\right) e^{-1/s_c} D_{\rm linear} \tag{40}$$

where $s_c = \xi/r_c$, and

$$\mathrm{EXP}_\ell(x) = \sum_{k=0}^{\ell} \frac{1}{k!} x^k. \tag{41}$$

The linear result is formally obtained by setting $n_c = 0$ or in the $d \to \infty$ limit. In the other extreme of $s \ll 1$ we get a VRH-like dependence

$$D \sim e^{-1/s_c}, \quad \text{for} \quad s \ll 1. \tag{42}$$

Numerical verification. To obtain an ERH estimate we have to fix the parameter n_c in Eq. (36). One approach is to regard it as a free fitting parameter. But it is of course better not to use any fitting parameters. Fortunately we know from [30,31] that $n_c = 4.5$ is the average number of bonds required to get percolation. The verification of the ERH estimate for the random site model with this value is demonstrated in Fig. 1(b).

X. ERH CALCULATION FOR THE MOTT HOPPING MODEL

We turn to calculating the ERH estimate for the nondegenerate Mott hopping model, and contrast it with the linear approximation, and with the traditional VRH estimate. The ERH threshold is determined through Eq. (29), leading to

$$w_c = w_0 \exp(-\epsilon_c), \tag{43}$$

$$\epsilon_c \equiv \left(\frac{d}{\Omega_d}\frac{n_c}{s^d}\right)^{1/(d+1)}. \tag{44}$$

In the VRH procedure the optimal hopping range is found by maximizing $w(r,\epsilon)$ along the tradeoff line of Eq. (33), as illustrated in Fig. 3, leading to

$$r^* = \left(\frac{d^2}{\Omega_d} n^* s\right)^{1/(d+1)} r_0, \tag{45}$$

and the associated rate is

$$w^* = w_c \quad \text{provided} \quad n^* = n_c/d. \tag{46}$$

This identification is necessary if we want the VRH to describe correctly the asymptotic dependence of D on s.

The calculation of the ERH integral of Eq. (30) is detailed in Appendix F. Thanks to our conventions the linear result is the same as Eq. (39), and the the final result can be written as follows:

$$D_{\mathrm{ERH}} = \mathrm{EXP}_{d+3}(\epsilon_c)\, e^{-\epsilon_c} D_{\mathrm{linear}}, \tag{47}$$

where $\mathrm{EXP}(x)$ is the polynomial defined in Eq. (41). The linear result is formally obtained by setting $\epsilon_c = 0$ or in the $d \to \infty$ limit.

We see that the VRH estimate can be regarded as an asymptotic approximation that holds for $s \ll 1$. Using Eqs. (15) and (16) we deduce from Eqs. (39) and (47) that

$$D_{\mathrm{linear}} \propto T, \tag{48}$$

while for $s \ll 1$,

$$D_{\mathrm{ERH}} \sim \left(\frac{1}{T}\right)^{2/(d+1)} \exp\left[-\left(\frac{T_0}{T}\right)^{1/(d+1)}\right], \tag{49}$$

where T_0 is a constant.

XI. ERH CALCULATION FOR THE BANDED QUASI-ONE-DIMENSIONAL MODEL

We can apply the ERH calculation also to the case of the quasi-one-dimensional model that we have studied in the past [18,19]. This model is motivated by studies of energy absorption [27]. For details see Appendix B. The network is defined by a banded matrix $\boldsymbol{w}$. For simplicity we assume that the sites are equally spaced and that the reason for the sparsity is the log-wide distribution of the in-band elements.

The ERH threshold w_c is deduced from Eq. (29). For a general $B(r)$ and $f(\epsilon)$ one can integrate over $d\epsilon$, and then it takes the form

$$\int_0^\infty \frac{\Omega_d\, r^{d-1} dr}{r_0^d}\, F\left[\log\left(\frac{w_0}{w_c} B(r)\right)\right] = n_c, \tag{50}$$

where $F(\epsilon)$ is the cumulative distribution function that corresponds to the density $f(\epsilon)$. Here we are considering a $d = 1$ network. However, we are dealing with a banded matrix which in some sense is like adding an extra (but bounded) dimension to the lattice.

Specifically we assume that $B(r) = 1$ within the band, and zero for $|r| > b$. The nonzero elements have a log-box distribution, namely, ϵ is distributed uniformly over a range $[0,\sigma]$. To have large σ means "sparsity." One should notice that this sparsity is less traumatic than having $s \ll 1$ in the $d = 1$ lattice model that we considered in Sec. IV. This is because the distribution is bounded from below by finite nonzero values. Accordingly we cannot have subdiffusion here.

We now turn to estimate D using the the ERH procedure. It should be clear that the success here is not guaranteed for reasons that we further discuss in the last paragraph of this section. From Eq. (50) it follows that $w_c = w_0 \exp(-\epsilon_c)$, where ϵ_c is the solution of

$$2bF(\epsilon_c) = n_c. \tag{51}$$

For the assumed ϵ distribution the solution of this equation is trivial

$$\epsilon_c = \frac{n_c}{2b}\sigma. \tag{52}$$

While doing the ERH integral of Eq. (30) note that the integral dr should be replaced by a sum. It is convenient to define

$$\tilde{b} \equiv \sum_{r=1}^{b} r^2 = \frac{1}{6} b(b+1)(2b+1). \tag{53}$$

Then the ERH estimate takes the form

$$D_{\mathrm{ERH}} = \frac{1}{\sigma}\left[\left(1 + \frac{n_c}{2b}\sigma\right) e^{-\frac{n_c}{2b}\sigma} - e^{-2\sigma}\right] \tilde{b} w_0. \tag{54}$$

The linear estimate of Eq. (28) is formally obtained by setting $n_c = 0$, and in the absence of disorder it obviously reduced to $D = \tilde{b} w_0$. We define

$$g_s = D/D_{\mathrm{linear}}. \tag{55}$$

Numerical results are presented in Fig. 4, and they agree with the ERH estimate.

At this point one wonders whether D can be extracted from the spectral analysis, i.e., via fitting to Eq. (20). In Fig. 4(c) we plot the D that is extracted from the spectral

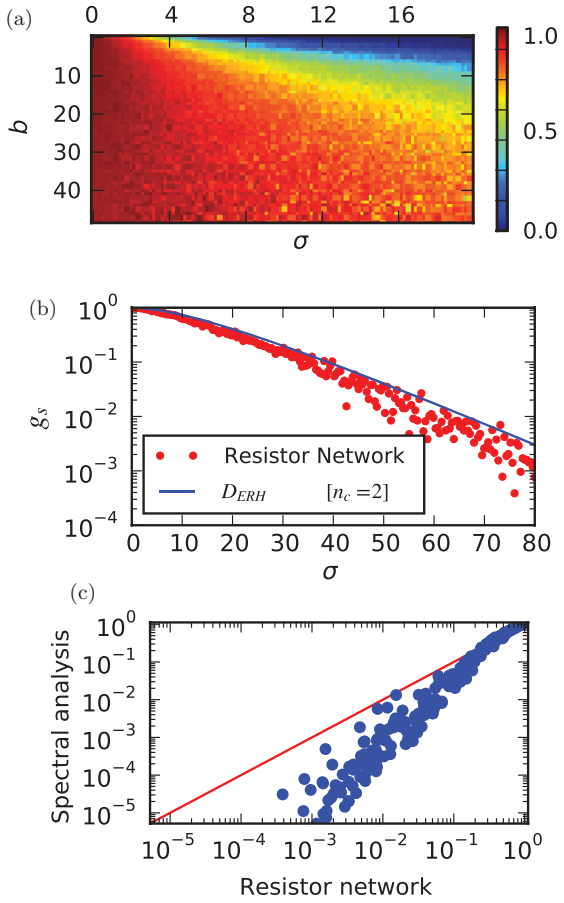

FIG. 4. (Color online) We consider a quasi $d = 1$ network that consists of $N = 1000$ sites with periodic boundary conditions. The network is described by a sparse banded matrix. The bandwidth is b, and the log-width of the rate distribution is σ. See text for details. (a) The numerical result for $g_s = D/D_{\text{linear}}$ imaged as a function of σ and b. The values of D are found via a numerical resistor network calculation, see Appendix A. (b) Subset of results that refer to the $b = 10$ matrix. The curve is the ERH prediction. (c) Scatter diagram shows the correlation between the D that was extracted from the spectral analysis and the D that was found via the resistor network calculation.

analysis versus the D that has been found via the resistor network calculation. We observe that the obtained values are much smaller. Our interpretation for that is as follows. The density of eigenvalues is related to the survival probability $\mathcal{P}(t)$ via a Laplace transform. For a quasi-one-dimensional system there is a short-time, $d = 2$ like, relatively fast transient. Consequently the $d = 1$ decay holds only asymptotically with a smaller prefactor. Accordingly we do not know whether there is a wise way to deduce D from the spectral analysis in the case of a quasi-one-dimensional network.

Concluding this section we would like to warn the reader that the use of the percolation picture in $d = 1$ is somewhat problematic: strictly speaking there is no percolation transition. Obviously for $b = 1$ we are back with the $d = 1$ lattice model for which there is subdiffusion if $s < s_{\text{cr}}$ with $s_{\text{cr}} = 1$. However, if b is reasonably large, it is not feasible to encounter such an anomaly in practice. Even if the distribution is not bounded from below, the redundancy due to $b > 1$ would lower the effective value of s_{cr}. Furthermore, in the Fermi-golden-rule picture (see next section) the occurrence of "weak links" along the band are practically not possible because the matrix elements V_{nm} are not uncorrelated random variables. We can refer to this as the *rigidity*. This rigidity is implied by semiclassical considerations.

XII. SEMILINEAR RESPONSE PERSPECTIVE

Considering models of energy absorption (see Appendix B), it is assumed that the transition rate w_{nm}, between unperturbed energy levels m and n, is determined by a driving source that has spectral content $\tilde{S}(\omega)$. The Fermi golden rule can be written as

$$w_{nm} = \tilde{S}(E_n - E_m)\,|V_{nm}|^2, \tag{56}$$

where V_{nm} is the perturbation matrix in the Hamiltonian. Accordingly we can write instead of $D = D[\boldsymbol{w}]$ an implied relation $D = D[\tilde{S}(\omega)]$. This relation is in general semilinear. This means that only the first property below, which corresponds to Eq. (8), is satisfied, not the second one.

$$D[\lambda\tilde{S}(\omega)] = \lambda\, D[\tilde{S}(\omega)], \tag{57}$$

$$D[\tilde{S}_a(\omega) + \tilde{S}_b(\omega)] = D[\tilde{S}_a(\omega)] + D[\tilde{S}_b(\omega)]. \tag{58}$$

To have a semilinear rather than linear response may serve as an experimental signature for the applicability of resistor-network modeling of energy absorption. We note, however, that if the the driving were added "on top" of a bath, the response would become linear at small intensities. Namely, if one substituted

$$\tilde{S}(\omega)_{\text{total}} = \tilde{S}_{\text{bath}}(\omega) + \tilde{S}(\omega), \tag{59}$$

it would be possible to linearize D with respect to the $\tilde{S}(\omega)$ of the driving source.

The statement that VRH is a "semilinear response" theory rather than "linear response" theory is a source for nonconstructive debates on terminology. The reason for the confusion about this point is related to the physical context. Do we calculate "current vs bias" or do we calculated "diffusion vs driving"? The response is linear in the former sense, but semilinear in the latter sense.

XIII. DISCUSSION

It should be clear that there are two major routes in developing a theory for D. Instead of deducing it from spectral properties as in [10], one can try to find ways to evaluate it directly via a resistor network calculation [7,12–15], leading in the standard Mott problem to the VRH estimate for D.

In [18,19,27] this approach was extended to handle "sparse" banded matrices whose elements have log-wide distribution, leading to a generalized VRH estimate. In this work we have pursued the same direction and obtained an improved estimate for D, the ERH estimate. Using this approach we showed that in the $d = 2$ case, as s becomes small, the functional $D[\boldsymbol{w}]$ exhibits a smooth crossover from linear behavior to semilinear VRH-type dependence.

Relation to other models. Disregarding the sparsity issue, the model that we were considering is a close relative of the Anderson localization problem. However, it is not the same

problem, and there are important differences that we would like to highlight. For the purpose of this discussion it is useful to be reminded that the hopping problem that we have addressed is essentially the same as studying the spectrum of vibrations in a disordered elastic medium. Hence $D^{1/2}$ parallels the speed of sound c of the Debye model. See Appendix D.

Mott vs Anderson. In the hopping model all the off-diagonal elements are positive numbers, while the negative diagonal elements compensate them. It follows that we cannot have "destructive interference," and therefore we do not have genuine Anderson localization. Consequently in general we might have diffusion, even in $d = 1$. In $d = 2$ we have a percolation threshold, which is again not like Anderson localization. See the discussion of fractons in [24].

Debye vs Anderson. In the standard Anderson model the eigenvalues form a band $\lambda \in [-\lambda_c, \lambda_c]$. The states at the edge of the band are always localized. The states in the middle of the band might be delocalized if $d > 2$. The spectrum that characterizes the hopping model does not have the same properties. With regard to the localization of vibrations in a disordered elastic medium [28], it has been found that the spectrum is $\lambda \in [0, \lambda_c]$. The ground state is always the $\lambda = 0$ uniform state. The localization length diverges in the limit $\lambda \to 0$. Consequently the Debye density of states is not violated: the spectrum is asymptotically the same as that of a diffusive (nondisordered) lattice. It follows that the survival probability should be like that of a diffusive system, and therefore we also expect, and get, diffusive behavior for the transport: spreading that obeys a diffusion equation.

XIV. SUMMARY

This work was originally motivated by the necessity to improve the resistor-network analysis of the diffusion in quasi-one-dimensional networks [18], and additionally from the desire to relate it to the recent RG studies [10] of the spectral properties of random site networks. The key issue that we wanted to address was the crossover from linear-like to semilinear dependence of D on the rates. This crossover show up as the "sparsity" of the system is varied.

It should be clear that unlike the RG-based expectation of [10], our analysis indicates that there is no subdiffusive behavior in $d = 2$. Accordingly, the anomalous $\log(t)$ spreading that is predicted in [10] should be regarded as a transient: for very small value of the sparsity parameter this transient might have a very long duration, but eventually normal diffusion takes over.

One can regard sparsity as an extreme type of disorder: the rates are distributed over many orders of magnitude. Still, unlike the $d = 1$ case, the implication of sparsity in $d = 2$ is not as dramatic: there is no phase transition between two different results, but a smooth crossover. It is therefore clear that our statements are consistent with those of older works that relate to the diverging localization properties of the low frequency vibrations in a disordered elastic medium [28].

The effective range hopping (ERH) procedure that we tested in this paper is a refinement of well-known studies of variable range hopping [7,11–15]. We used the insight of [7,13,14] that connects VRH with the theory of percolation.

Disregarding possible inaccuracy in the determination of the optimal rate, the ERH calculation provides a *lower* bound for D. Accordingly, by obtaining a nonzero result it is rigorously implied that D is finite. The purpose of the numerics was to demonstrate that in practice the outcome of the ERH calculation provides a very good estimate of the actual result, interpolating very well the departure from linearity.

It was important for us to clarify that a large class of networks can be treated *on an equal footing*. In particular we demonstrated that the application of the ERH estimate does not require any fitting parameters. We have verified that the same prescription can be applied to both the $d = 2$ lattice model and the $d = 2$ random site model, provided one uses the appropriate percolation threshold that is known from percolation theory.

For the traditional Mott hopping model and its degenerated version we obtained the refined expressions Eq. (47) and Eq. (40), respectively. In these expressions the *full* dependence on the dimensionality (d) is explicit, and the crossover to a linear response as a function of the sparsity (s) is transparent. Note that in the degenerate random site model the sparsity is merely a geometrical feature, while in the nondegenerate Mott model the sparsity depends on the temperature as implied by Eq. (16).

We would like to reemphasize that the original motivation for this work was the study of energy absorption by driven mesoscopic systems. In this context the implication of the semilinear crossover is the breakdown of linear response theory. The latter issue has been extensively discussed in past publications [27].

ACKNOWLEDGMENTS

We thank Amnon Aharony, Ariel Amir, Ora Entin-Wohlman, Rony Granek, and Joe Imry for illuminating discussions, comments, and references. This work has been supported by the Israel Science Foundation.

APPENDIX A: LATTICE MODEL WITH N.N. HOPPING

For $s \ll 1$ the $d = 1$ random site model is essentially equivalent to a lattice model with equally spaced sites, near-neighbor transitions, and random ϵ. From the identification $\epsilon = r/\xi$ it follows that the distribution of the "activation energy" is

$$f(\epsilon) = s \exp(-s\epsilon), \quad s \equiv \xi/r_0. \tag{A1}$$

This implies that the the distribution of the rates is

$$\tilde{f}(w)dw = \frac{s\, w^{s-1} dw}{w_0^s}[w < w_0]. \tag{A2}$$

The density of sites to which a transition can occur is

$$\rho(r,\epsilon) = c_L \delta(r - r_0)\ f(\epsilon), \tag{A3}$$

where $c_L = 2$ is the coordination number. This corresponds to the $d = 1$ case of Eq. (12).

The $d = 2$ version of the lattice model has no strict relation to the $d = 2$ random site model. A popular choice is to assume a box distribution for the activation energy within some interval $0 < \epsilon < \sigma$. The density of sites to which a transition can occur is $2\pi r f(\epsilon)$ for large r, as implied by Eq. (12). But for small r

the effective density is given by Eq. (A3) with the coordination number $c_L = 4$.

APPENDIX B: QUASI-ONE-DIMENSIONAL BANDED MATRIX MODEL

On equal footing we consider the quasi-one-dimensional banded lattice model. This model is motivated by studies of energy absorption [27]. In this context the transition rates are determined by the Fermi golden rule (FGR). Hence we write

$$w_{nm} = w_0\, e^{-\epsilon_{nm}}\, B(E_n - E_m). \tag{B1}$$

Here n and m are unperturbed energy levels of the system, but we shall keep calling them "sites" in order to avoid duplicate terminology. The density of sites relative to some initial site is characterized by the same joint distribution function as for the $d = 1$ network,

$$\rho(r,\epsilon) = 2f(\epsilon). \tag{B2}$$

Here $r = |E_n - E_m|$ is the distance between the energy levels, which is formally analogous to $r = |x_n - x_m|$ in the random site hopping model. We use here units such that the mean level spacing is unity. In the later numerical analysis we assume equally spaced levels such that the distance is simply $r = |n - m|$.

In the physical context the band profile $B(r)$ is determined by the semiclassical limit, while the distribution of the ϵ values is implied by the intensity statistics of the matrix elements. This intensity statistics is known as Porter-Thomas in the strongly chaotic case, corresponding to the Gaussian ensembles, but it becomes log-wide for systems with "weak quantum chaos" [19], reflecting the sparsity that shows up in the limiting case of integrable system [32].

In the numerical analysis we have considered simple banded matrices for which $B(r) = 1$ for $r \leqslant b$, and zero otherwise. Accordingly $1 + 2b$ is the bandwidth. The elements within the band are log-box distributed: this means that ϵ is distributed uniformly over a range $[0,\sigma]$. Note that log-box distribution is typical of glassy systems, where the tunneling rate depends exponentially on the distance between the sites.

APPENDIX C: NUMERICAL EXTRACTION OF D

In a diffusive system the coarse-grained spreading is described by the standard diffusion equation, with an evolving Gaussian distribution

$$\rho(x;t) = \prod_{i=1}^{d} \frac{1}{\sqrt{2\pi\, S_x(t)}} \exp\left[-\frac{x_i^2}{2S_x(t)}\right], \tag{C1}$$

where $S_x(t) = 2Dt$. It follows from this expression that

$$S(t) = \langle r^2(t)\rangle = (2d)Dt. \tag{C2}$$

Starting with all the probability concentrated in one unit cell we get for the survival probability

$$\mathcal{P}(t) \sim \frac{r_0^d}{(4\pi\, Dt)^{d/2}}. \tag{C3}$$

The eigenvalues of the diffusion equation are

$$\lambda_k = Dq_k^2, \quad k = \text{index}, \tag{C4}$$

where the possible values of the momentum are determined by the periodic boundary conditions as $q = (2\pi/L)\vec{k}$. It follows that the cumulative number of eigenstates per site is

$$\mathcal{N}(\lambda) = \left(\frac{r_0}{2\pi}\right)^d \frac{\Omega_d}{d}\left[\frac{\lambda}{D}\right]^{d/2}. \tag{C5}$$

It is well known that the survival probability is related to the eigenvalues of $\boldsymbol{w}$ through the relation

$$\mathcal{P}(t) = \frac{1}{N}\sum_{\lambda} e^{-\lambda t} \equiv \int_0^\infty g(\lambda)d\lambda\, e^{-\lambda t}. \tag{C6}$$

For a diffusive system one can verify that the expressions above for $g(\lambda)$ and $\mathcal{P}(t)$ are indeed related by a Laplace transform. More generally, it follows that D can be deduced from the asymptotic behavior of $g(\lambda)$ in the $\lambda \to 0$ limit where the diffusive description is valid. In contrast to that for large λ, we expect $g(\lambda)$ to coincide with the distribution of the decay rates $\gamma_n = \sum_m w_{mn}$, reflecting localized modes.

APPENDIX D: RELATION TO DEBYE MODEL

Consider a system of unit masses that are connected by springs. Once can describe the system by a matrix $\boldsymbol{w}$ whose off-diagonal elements w_{nm} are the spring constants. The eigenfrequencies are determined accordingly, namely, $\omega_k = \sqrt{\lambda_k}$. Assuming that the low lying modes are like acoustic phonons with dispersion $\omega = c|q|$, where c is the so-called speed of sound, one deduces that

$$\omega_k = c|q_k|, \quad k = \text{index}, \tag{D1}$$

Consequently the associated counting function is as in the Debye model:

$$\mathcal{N}(\omega) = \left(\frac{r_0}{2\pi\, c}\right)^d \frac{\Omega_d}{d}\, \omega^d. \tag{D2}$$

Comparing the above expressions with Eqs. (C4) and (C5) it follows that the calculation of c^2 is formally the same as the calculation of D.

APPENDIX E: RESISTOR NETWORK CALCULATION

The diffusion coefficient D is formally like the calculation of the conductivity of the network. Therefore it can be determined via a numerical solution of a circuit equation. It is convenient to use the language of electrical engineering to explain how the resistor network calculation is carried out in practice. Accordingly we use in this appendix the notation $\boldsymbol{G}$ instead of $\boldsymbol{w}$ for the matrix that describes the resistor network, and σ instead of D for its conductivity. We define a vector $\boldsymbol{V} = \{V_n\}$, where V_n is the voltage at node n, analogous to p_n. We also define a vector $\boldsymbol{I} = \{I_n\}$ of injected currents. The Kirchhoff equation [Eq. (1)] for a steady state can be written as $\boldsymbol{GV} = 0$.

If the nodes were connected to external "reservoirs" the Kirchhoff equation would take the form $\boldsymbol{GV} = \boldsymbol{I}$. The matrix $\boldsymbol{G}$ has an eigenvalue zero which is associated with a uniform voltage eigenvector. Therefore, it has a pseudo-inverse rather than an inverse, and consequently the Kirchhoff equation has a solution if and only if the net current is $\sum_n I_n = 0$.

For the purpose of calculating the conductivity we add a source $I_1 = -1$ and a drain $I_2 = 1$. We select the location of the source (site 1) and the drain (site 2) away from the endpoints. From the solution of the Kirchhoff equation we deduce

$$\sigma[d=1] = [(V_2 - V_1)/L]^{-1}, \tag{E1}$$

where L is the distance between the contacts.

With regard to the quasi-one-dimensional model, we take the distance between the contacts to be $L' = N/2$ and look at the voltage drop along an inner segment of length $L = L' - 2b$, to avoid the transients at the contact points.

To find the conductivity in the $d = 2$ case we select contacts points that have distance $L \sim (N/2)^{1/2}$, and use the formula

$$\sigma[d=2] = [(V_2 - V_1)/\ln(L/\ell)]^{-1}, \tag{E2}$$

where $\ell \sim 1$ is the shift of the measurement point from the contact point. Here the voltage drop is divided by $\ln(L/\ell)$ instead of L, reflecting the two-dimensional geometry of the flow.

APPENDIX F: CALCULATION OF THE ERH INTEGRAL

The calculation of the ERH integral for the random site model involved the incomplete Γ function [33]

$$\Gamma(\ell{+}1,x) = \int_0^x r^\ell e^{-r} dr = \ell!\,\mathrm{EXP}_\ell(x)\, e^{-x}. \tag{F1}$$

We first consider the degenerate Mott model. We substitute in Eq. (30), the $w(r,\epsilon)$ of Eq. (4), and the $\rho(r,\epsilon)$ of Eq. (12) with Eq. (14). Thanks to the $\delta(\epsilon)$ we are left just with a dr integration that is split into the domains $0 < r < r_c$ and $r > r_c$. Namely,

$$\begin{aligned} D_{\mathrm{ERH}} &= \frac{w_0\Omega_d}{2d}\int_0^{r_c} e^{-r_c/\xi}\frac{r^{d+1}}{r_0^d}dr \\ &\quad + \frac{w_0\Omega_d}{2d}\int_{r_c}^{\infty} e^{-r/\xi}\frac{r^{d+1}}{r_0^d}dr \\ &= \frac{w_0\Omega_d}{2d} e^{-r_c/\xi}\frac{r_c^{d+2}}{d+2}\frac{1}{r_0^d} \\ &\quad + \frac{w_0\Omega_d}{2d}\frac{\xi^{d+2}}{r_0^d}\Gamma\left(d+2,\frac{r_c}{\xi}\right) \\ &= \frac{w_0\Omega_d\xi^{d+2}}{2d(d+2)r_0^d}\Gamma\left(d+3,\frac{r_c}{\xi}\right). \end{aligned} \tag{F2}$$

This leads directly to Eq. (40) with Eq. (39).

Turning to the nondegenerate Mott model we have to deal with a two-dimensional integral $dr\,d\epsilon$ that has, as in the previous case, two domains $w > w_c$ and $0 < w < r_c$. The two domains are separated by the line $\epsilon + (r/\xi) = \epsilon_c$. It is therefore natural to change variables:

$$x = \epsilon + (r/\xi), \tag{F3}$$

$$y = \tfrac{1}{2}[-\epsilon + (r/\xi)], \tag{F4}$$

hence

$$\begin{aligned} D_{\mathrm{ERH}} &= \frac{w_0\Omega_d}{2dr_0^d}\int_0^{\epsilon_c}\xi dx\int_{-x/2}^{x/2} dy\, e^{-\epsilon_c}\left(\xi y + \xi\frac{x}{2}\right)^{d+1} \\ &\quad + \frac{w_0\Omega_d}{2dr_0^d}\int_{\epsilon_c}^{\infty}\xi dx\int_{-x/2}^{x/2} dy\, e^{-x}\left(\xi y + \xi\frac{x}{2}\right)^{d+1} \\ &= \frac{w_0\Omega_d}{2dr_0^d}\xi^{d+2}e^{-\epsilon_c}\frac{\epsilon_c^{d+3}}{(d+2)(d+3)} \\ &\quad + \frac{w_0\Omega_d}{2dr_0^d(d+2)}\xi^{d+2}\,\Gamma(d+3,\epsilon_c) \\ &= \frac{w_0\Omega_d\xi^{d+2}}{2d(d+2)(d+3)r_0^d}\Gamma(d+4,\epsilon_c). \end{aligned} \tag{F5}$$

This leads directly to Eq. (47) with Eq. (39).

[1] S. N. Dorogovtsev, A. V. Goltsev, J. F. F. Mendes, and A. N. Samukhin, Phys. Rev. E **68**, 046109 (2003).

[2] S. Bradde, F. Caccioli, L. Dall'Asta, and G. Bianconi, Phys. Rev. Lett. **104**, 218701 (2010).

[3] J.-P. Bouchaud and A. Georges, Phys. Rep. **195**, 127 (1990).

[4] H. Scher and E. W. Montroll, Phys. Rev. B **12**, 2455 (1975).

[5] D. Kaya, N. L. Green, C. E. Maloney, and M. F. Islam, Science **329**, 656 (2010).

[6] D. Stauffer and A. Aharony, *Introduction to Percolation Theory* (CRC, Boca Raton, FL, 1994)

[7] B. I. Halperin, Physica D **38**, 179 (1989).

[8] S. R. Nagel, A. Rahman, and G. S. Grest, Phys. Rev. Lett. **47**, 1665 (1981).

[9] W. Schirmacher and M. Wagener, Philos. Mag. B **65**, 607 (1992).

[10] A. Amir, Y. Oreg, and Y. Imry, Phys. Rev. Lett. **105**, 070601 (2010); Phys. Rev. B **77**, 165207 (2008).

[11] N. F. Mott, Philos. Mag. **22**, 7 (1970); N. F. Mott and E. A. Davis, *Electronic Processes in Non-crystalline Materials* (Clarendon, Oxford, 1971).

[12] A. Miller and E. Abrahams, Phys. Rev. **120**, 745 (1960).

[13] V. Ambegaokar, B. Halperin, and J. S. Langer, Phys. Rev. B **4**, 2612 (1971).

[14] M. Pollak, J. Non-Cryst. Solids **11**, 1 (1972).

[15] B. I. Shklovskii and A. L. Efros, *Electronic Properties of Doped Semiconductors* (Springer-Verlag, Berlin, 1984).

[16] A. Aharony, E. I. Hinrichsen, A. Hansen, J. Feder, T. Jossang, and H. H. Hardy, Physica A **177**, 260 (1991).

[17] L. Hinrichsen, A. Aharony, J. Feder, A. Hansen, T. Jossang, and H. H. Hardy, Transp. Porous Media **12**, 55 (1993).

[18] S. Bandopadhyay, Y. Etzioni, D. Cohen, Europhys. Lett. **76**, 739 (2006); D. Cohen, Phys. Rev. B **75**, 125316 (2007); A. Stotland, T. Kottos, and D. Cohen, *ibid.* **81**, 115464 (2010).

[19] A. Stotland, D. Cohen, and N. Davidson, Europhys. Lett. **86**, 10004 (2009); A. Stotland, L. M. Pecora, and D. Cohen, *ibid.* **92**, 20009 (2010); Phys. Rev. E **83**, 066216 (2011).

[20] S. Alexander, J. Bernasconi, W. R. Schneider, and R. Orbach, Rev. Mod. Phys. **53**, 175 (1981).

[21] S. Havlin, D. Movshovitz, B. Trus, and G. H. Weiss, J. Phys. A **18**, L719 (1985).

[22] R. Granek and J. Klafter, Phys. Rev. Lett. **95**, 098106 (2005).
[23] S. Reuveni, R. Granek, and J. Klafter, Proc. Natl. Acad. Sci. **107**, 13696 (2010); Phys. Rev. E **81**, 040103 (2010).
[24] D. Ben-Avraham and S. Havlin, *Diffusion and Reactions in Fractals and Disordered Systems* (Cambridge University, New York, 2000).
[25] A. Klemm, R. Metzler, and R. Kimmich, Phys. Rev. E **65**, 021112 (2002).
[26] F. Camboni and I. M. Sokolov, Phys. Rev. E **85**, 050104(R) (2012).
[27] For a review and further references, see D. Cohen, arXiv:1202.5871.
[28] K. Ishii, Prog. Theor. Phys. Suppl. **53**, 77 (1973); S. John, H. Sompolinsky, and M. J. Stephen, Phys. Rev. B **27**, 5592 (1983); W. Kantelhardt and A. Bunde, Phys. Rev. E **56**, 6693 (1997); Q. Li, C. M. Soukoulis, and G. S. Grest, Phys. Rev. B **41**, 11713 (1990).
[29] A. Amir, J. J. Krich, V. Vitelli, Y. Oreg, and Y. Imry, arXiv:1209.2169.
[30] N. W. Dalton, C. Domb, and M. F. Sykes, Proc. Phys. Soc. **83**, 496 (1964).
[31] G. E. Pike and C. H. Seager, Phys. Rev. B **10**, 1421 (1974).
[32] T. Prosen and M. Robnik, J. Phys. A **26**, L319 (1993); E. J. Austin and M. Wilkinson, Europhys. Lett. **20**, 589 (1992); Y. Alhassid and R. D. Levine, Phys. Rev. Lett. **57**, 2879 (1986); Y. V. Fyodorov, O. A. Chubykalo, F. M. Izrailev, and G. Casati, *ibid.* **76**, 1603 (1996).
[33] *NIST Handbook of Mathematical Functions*, edited by F. W. J. Olver, D. W. Lozier, R. F. Boisvert, and C. W. Clark (Cambridge University Press, New York, NY, 2010), Eqs. (8.4.8) and (8.4.11), http://dlmf.nist.gov.

Appendix B

Spacing Statistics in d-dimensions

Some clarifing points regarding the statistics of uniformly distributed sites will be made in this section.

There are N sites distributed randomly within a d-dimensional hypercube of volume L^d. We define a typical length r_0 by:

$$\frac{L^d}{r_0^d} \;=\; N \tag{B.1}$$

From now on we shall ignore boundary conditions, assuming N is large enough. In the numerics we have used periodic boundary conditions.

If we choose some arbitrary point as the origin, the distribution of sites around this point will be:

$$\rho(r)dr = \frac{\Omega_d r^{d-1}}{r_0^d}dr \tag{B.2}$$

Where Ω_d is the d dimensional solid angle:

$$\Omega_d \;=\; 2,\; 2\pi,\; 4\pi, \ldots \tag{B.3}$$

The distribution of the nearest neighbor distance can be derived [27], using a differential equation.

Let us denote by $P(r)$ the probability that the first near neighbor will be between r and $r + dr$. The probability of having no neighbors up to distance r is

$$P_0(r) \;=\; 1 - \int_0^r P(r)dr \tag{B.4}$$

$P(r)$ must equal the probability of having no neighbors up to distance r times the probabilty of finding a neighbor between r and $r + dr$. So $P(r)$ must satisfy:

$$P(r) = P_0(r) \times \rho(r) = \left[1 - \int_0^r P(r)dr\right] \rho(r) \tag{B.5}$$

$$\frac{P(r)}{\rho(r)} = 1 - \int_0^r P(r)dr \tag{B.6}$$

$$\frac{d}{dr}\left(\frac{P(r)}{\rho(r)}\right) = -\rho(r)\frac{P(r)}{\rho(r)} \tag{B.7}$$

Which has the solution:

$$P(r) = \rho(r)\mathrm{e}^{-\int_0^r \rho(r)dr} \tag{B.8}$$

$$= \frac{\Omega_d r^{d-1}}{r_0^d}\mathrm{e}^{-\frac{\Omega_d}{d}\left(\frac{r}{r_0}\right)^d} \tag{B.9}$$

Where in the last step we have plugged in $\rho(r)$ from Equation B.2

Appendix C

Resistor Network Computation

C.1 Resistor network calculation of transport

The transmission rates of our model are analogous to conductors. The conductance of the entire system can be derived using Kirchoff's laws. We define a vector $\boldsymbol{V} = \{v_n\}$, for the voltage of each site (analogous to p_n), and a vector $\boldsymbol{I} = \{I_n\}$ for outside current going into the site. The Kirchoff equation takes the form

$$\boldsymbol{I} \;=\; \boldsymbol{G} \cdot \boldsymbol{V} \tag{C.1}$$

Where $\boldsymbol{G} = \boldsymbol{W}$.

We can then add a source $I_s = -1$ and a drain $I_d = 1$, setting the rest of the currents to zero. By numerically solving the above linear equation for $\boldsymbol{V}$, we can extract the conductivity. For practical reasons we have chosen sites that are far away from each other but not on the edges, and we have also looked on the voltage drop along an inner segment, to avoid the transients at the contact points.

In the d=1 case, the conductance is simply the conductivity multiplied by the distance between the points.

For the d=2 case read the following section.

C.2 Point terminal resistivity in d=2

When discussing resistivity in a square $2d$ sample, it is common to treat two opposite edeges of the sample as terminals. In this setting, the *resistance* between the terminals equals the

resistivity of the material. However, for our calculation, it is easier to use point contacts as terminals. Therefore we present the derivation of the relation between resistance and resistivity in this case. We will assume the system is homgenous in space and as large as required.

We put a point contact source of radius r_0 at the origin, so that the current spreads to infinity with radial symmetry. The current density will therefore be

$$J = \frac{I}{2\pi r} \tag{C.2}$$

The electric field and voltage are then

$$E = \rho J = \rho \frac{I}{2\pi r} \tag{C.3}$$

$$V = \int_{r_0}^{r} E dr' = \rho \frac{I}{2\pi} \ln \frac{r}{r_0} \tag{C.4}$$

Here ρ stands for the resistivity. We now use superposition to add a sink of radius r_0 at distance r from the origin. Due to the symmetry of the problem, the voltage just doubles. The resistance is now:

$$R = \frac{V}{I} = \frac{\rho}{\pi} \ln \frac{r}{r_0} \tag{C.5}$$

$$\rho = \frac{\pi}{\ln \frac{r}{r_0}} R \tag{C.6}$$

In order to find ρ we compute R numerically.

C.3 Some analysis of banded matrices

To "get a feeling" of the expected spectrum of a banded matrix, we have looked at the spectrum of a perfectly ordered matrix.

$$w_{ij} = \begin{cases} 1 & \text{if } |i-j| \leq b \\ -2b & \text{if } i = j \\ 0 & \text{otherwise} \end{cases} \tag{C.7}$$

The analytical eigenvalues are:

$$\lambda = -2 \sum_{n=1..b} (\cos(n \cdot k) - 1) \tag{C.8}$$

$$k = \frac{2\pi m}{N} \tag{C.9}$$

Appendix D

Numerical Routines

For the numerical calculations, we have used python 2.6 [28], together with the scipy [29] package for numerics and the matplotlib [30] package for graphics. The source files are available online at : http://physweb.bgu.ac.il/~jarondl/LINKS/MSc_FILES/.

The source files are packaged into a standard python package, and can be installed as any other package. If a package manager is installed (e.g. pip), one should use it, as in :

```
pip install --user http://physweb.bgu.ac.il/~jarondl/LINKS/MSc_FILES/jarondl_msc-1.0.t
```

If not, the package should be extracted, and the "setup.py" script can be used:

```
python setup.py install --user
```

After this installation, the jarondl_msc package will be available, including the following modules:

```
ptsplot  geometry  plotdl  sparsedl
```

The `ptsplot` module is the main file of the package. The three other files contain sub-routines and class defentions used in `ptsplot`.

To reproduce all of the plots used in this proposal, one can simply run:

```
python -m jarondl_msc.ptsplot
```

If the files `D_banded.npz, D_banded_b10.npz` and `D_2d.npz` (available online) exist in the same directory as where the script is run, this data will be used. Otherwise, the numerics will run first, and then the plots will be made. This might take several hours, depending on the computer.

Bibliography

[1] A. Kolmogoroff, "Zur theorie der markoffschen ketten," Mathematische Annalen **112**, 155 (1936).

[2] P. W. Anderson, "Absence of diffusion in certain random lattices," Physical Review **109**, 1492 (1958).

[3] J. T. Edwards and D. J. Thouless, "Numerical studies of localization in disordered systems," Journal of Physics C: Solid State Physics **5**, 807 (1972).

[4] D. Thouless, "Electrons in disordered systems and the theory of localization," Physics Reports **13**, 93 (1974).

[5] D. Braun, E. Hofstetter, A. MacKinnon, and G. Montambaux, "Level curvatures and conductances: A numerical study of the thouless relation," Physical Review B **55**, 7557 (1997).

[6] R. Kubo, "Statistical-mechanical theory of irreversible processes. i. general theory and simple applications to magnetic and conduction problems," Journal of the Physical Society of Japan **12**, 570 (1957).

[7] O. Narayan and S. Ramaswamy, "Anomalous heat conduction in one-dimensional momentum-conserving systems," Physical Review Letters **89**, 200601 (2002).

[8] A. Dhar, "Heat conduction in the disordered harmonic chain revisited," Physical Review Letters **86**, 5882 (2001).

[9] S. Lepri, R. Livi, and A. Politi, "On the anomalous thermal conductivity of one-dimensional lattices," Europhysics Letters (EPL) **43**, 271 (1998).

[10] A. V. Savin, G. P. Tsironis, and A. V. Zolotaryuk, "Heat conduction in one-dimensional systems with hard-point interparticle interactions," Physical Review Letters **88**, 154301 (2002).

[11] L. Delfini, S. Lepri, R. Livi, and A. Politi, "Comment on Equilibration and universal heat conduction in fermi-pasta-ulam chains," Physical Review Letters **100**, 199401 (2008).

[12] A. Dhar and O. Narayan, "Dhar etal. reply:," Physical Review Letters **100**, 199402 (2008).

[13] L. Wang and T. Wang, "Power-law divergent heat conductivity in one-dimensional momentum-conserving nonlinear lattices," EPL (Europhysics Letters) **93**, 54002 (2011).

[14] P. Tong, B. Li, and B. Hu, "Wave transmission, phonon localization, and heat conduction of a one-dimensional frenkel-kontorova chain," Physical Review B **59**, 8639 (1999).

[15] S. Lepri, R. Livi, and A. Politi, "Thermal conduction in classical low-dimensional lattices," arXiv:cond-mat/0112193 (2001), phys. Rep. volume 377(1) (April 2003) pp. 1-80.

[16] R. F. Joshua D. Bodyfelt, Mei C. Zheng and T. Kottos, "Scaling theory of heat transport in quasi-1d disordered harmonic chains," Submitted.

[17] L. Erdos, A. Knowles, H.-T. Yau, and J. Yin, "The local semicircle law for a general class of random matrices," arXiv:1212.0164 (2012).

[18] Y. V. Fyodorov and A. D. Mirlin, "Scaling properties of localization in random band matrices: A -model approach," Physical Review Letters **67**, 2405 (1991).

[19] E. P. Wigner, "Characteristic vectors of bordered matrices with infinite dimensions," Annals of Mathematics. Second Series **62**, 548564 (1955).

[20] Y. de Leeuw and D. Cohen, "Diffusion in sparse networks: linear to semi-linear crossover," arXiv:1206.2495 (2012).

[21] S. Alexander, J. Bernasconi, W. R. Schneider, and R. Orbach, "Excitation dynamics in random one-dimensional systems," Reviews of Modern Physics **53**, 175 (1981); A. Amir, Y. Oreg, and Y. Imry, "Localization, anomalous diffusion, and slow relaxations: A random distance matrix approach," Physical Review Letters **105**, 70601 (2010).

[22] A. Stotland, T. Kottos, and D. Cohen, "Random-matrix modeling of semilinear response, the generalized variable-range hopping picture, and the conductance of mesoscopic rings," Physical Review B **81**, 115464 (2010).

[23] R. L. Blumberg Selinger, S. Havlin, F. Leyvraz, M. Schwartz, and H. E. Stanley, "Diffusion in the presence of quenched random bias fields: A two-dimensional generalization of the sinai model," Physical Review A **40**, 6755 (1989).

[24] P. M. Richards, "Theory of one-dimensional hopping conductivity and diffusion," Physical Review B **16**, 1393 (1977).

[25] P. K. Hung, T. V. Mung, and N. V. Hong, "Diffusion in one-dimensional disordered lattice," Modern Physics Letters B **26**, 1150011 (2012).

[26] A. Amir, Y. Oreg, and Y. Imry, "Mean-field model for electron-glass dynamics," Physical Review B **77**, 165207 (2008).

[27] P. Hertz, "ber den gegenseitigen durchschnittlichen abstand von punkten, die mit bekannter mittlerer dichte im raume angeordnet sind," Mathematische Annalen **67**, 387 (1909); S. Chandrasekhar, "Stochastic problems in physics and astronomy," Reviews of Modern Physics **15**, 1 (1943); S. Torquato, B. Lu, and J. Rubinstein, "Nearest-neighbor distribution functions in many-body systems," Physical Review A **41**, 2059 (1990).

[28] {Guido van Rossum}, "{Python}," .

[29] E. Jones, {Travis, Oliphant}, {Pearu, Peteron}, and {Others}, "{SciPy}: open source scientific tools for {Python}," (2001).

[30] J. Hunter, "Matplotlib: A 2D graphics environment," Computing in Science & Engineering **9**, 90 (2007).